IEEE Access
Multidisciplinary ⋮ Rapid Review ⋮ Open Access Journal

Received December 1, 2020, accepted December 20, 2020, date of publication December 31, 2020,
date of current version January 13, 2021.

Digital Object Identifier 10.1109/ACCESS.2020.3048346

Wideband Low-Profile Ku-Band Transmitarray Antenna

MEI-YU LI, YONG-LING BAN, (Member, IEEE), AND FU-QIANG YAN
School of Electronic Science and Engineering, University of Electronic Science and Technology of China, Chengdu 611731, China

Corresponding author: Yong-Ling Ban (byl@uestc.edu.cn)

This work was supported by the National Natural Science Foundation of China under Grant 61971098 and Grant U19A2055.

ABSTRACT A wideband, low profile transmitarray antenna (TA) operating in Ku-band (12GHz-18GHz) is proposed. The transmitarray antenna is composed of aperiodic transmitarray units arranged periodically. The TA unit is mainly composed of three layers, which are composed of metals and substrates. Square patches are printed on the substrate of the top and bottom layers, and the middle layer is a Jerusalem slot in the ground. The overall thickness of TA unit is $0.165\lambda_0$ (λ_0 is the free space wavelength at 15GHz). In Ku-band, the insertion of the TA unit is less than 0.5dB, which reduces the backward radiation of the transmitarray antenna. The 360° phase is achieved by changing the length of the patch and slot, and the proposed transmitarray unit has a flat phase curve and great transmission characteristics. In order to verify the proposed design, a transmitarray antenna with 351 TA units operating at 15GHz is fabricated and measured. The measurement results show that the TA can achieve a 37.3% (14.4GHz-20GHz) 1-dB gain bandwidth, the measurement gain is 23.06dBi with 42.3% aperture efficiency at 15GHz, and the backward radiation level is below -15dB. The designed TA unit has symmetrical structure, so the transmitarray antenna can work in dual linear polarization or dual circular polarization.

INDEX TERMS Transmitarray antenna, wideband, dual-polarization, low-profile.

I. INTRODUCTION

Transmitarray antenna is a planar structure, which combines the advantages of lens antenna. Compared with other high gain antennas, it has the advantages of low processing cost, simple feeding and flexible functions, so it can be applied to radar, satellite communication, wireless systems [1]–[3], etc. Compared with the reflectarray antenna, its feed and radiation fields are on both sides of the array respectively, so there is no feed blockage effect. However, due to the narrow band limitation of the transmitarray unit and the different spatial phase delays at different frequencies, the transmitarray antenna has a narrow bandwidth.

Recent studies have proposed many approaches to expand the operating frequency band of transmitarray antenna, which can be divided into the following three ways. The first and most popular approach is the multilayer frequency selective surface (M-FSS) [4]–[11]. The TA units at different positions of the transmitarray have the same structure shape, but different sizes, which are calculated according to the phase compensation of the units at that position. In [9], a semiplaner transmitarray is proposed, which maintains a certain geometric curvature to expand the gain bandwidth of the array. The 1-dB gain bandwidth is 24.27%, the aperture efficiency is 62%, and the overall thickness of the transmitarray is $0.61\lambda_0$. In this approach, the phase of 360° is obtained by introducing $1/4\lambda_0$ air layer, so the profile of transmitarray antenna is high. The second is receive/transmit approach [2], [12]–[15], which is mainly composed of three layers, the receiving / transmitting layers and the middle phase-shifting layer. The phase compensation is realized by changing the phase shift of the intermediate layer. In [15], a D-band (110-170GHz) wideband transmitarray with high gain and high-efficiency based on low-temperature co-fired ceramic technology is proposed, which can achieve a 3-dB gain bandwidth of 24.29% (124-158GHz), the measured peak gain is 33.45dBi at 150GHz with the aperture efficiency is 44.03%, and the overall thickness of the transmitarray is $0.2\lambda_0$. This approach cancels the air layer and reduces the overall thickness, but the insertion loss of transmitarray unit is high. The third is rotation angle approach [16]–[21]. The shape of transmitarray unit at each position in the transmitarray is the same, and phase compensation is realized by rotating the transmitarray unit. In [21], the performance of the transmitarray is effectively improved by rotating the intermediate layer

The associate editor coordinating the review of this manuscript and approving it for publication was Lu Guo.

and optimizing the phase compensation, which can achieve 21.5% 1-dB gain bandwidth, 40% aperture efficiency, and the overall thickness of the array is $0.127\lambda_0$. The transmitarray based on rotation angle can only work in single polarization.

There are also some other approaches to solve the problem of narrow bandwidth and high profile of transmitarray antenna. In [22], the phase distribution of the transmitarray is optimized by calculating the average unit loss under different central unit phase values to achieve high-performance transmission. The 1-dB gain bandwidth is 9%, the 3-dB gain bandwidth is 19.4%, the aperture efficiency is 30%, and the overall thickness of the transmitarray is $0.51\lambda_0$. In [23], [24], a hybrid design method is proposed to realize the ultra-thin transmitarray, which uses no less than two types of units to cover the 360° phase, and reduce the profile of the transmitarray. In [23], the 1-dB gain bandwidth is 6.7%, the aperture efficiency is 30%, and the overall thickness of the transmitarray is $0.07\lambda_0$. In [24], four metal cylinders are used to achieve the maximum transmission amplitude, which can achieve the 1-dB gain bandwidth of 9.6%, the aperture efficiency of 40%, and the overall thickness of the transmitarray is $0.14\lambda_0$.

The transmitarray unit designed in this article introduces an ultra-thin air layer and a multi-resonant structure to expand the operating frequency band and reduce the backward radiation of the transmitarray. Since the proposed wideband transmitarray unit has a completely symmetrical structure, the wideband transmitarray can work in dual linear polarization or dual circular polarization. This article is organized as follows. The detailed configuration of the proposed wideband transmitarray unit is first presented in Section II. The evolution and basic working mechanism of the unit are discussed. The simulation results and measurement results of the transmitarray are analyzed in Section III. Finally, the conclusions are given in section IV.

II. DESIGN OF THE WIDEBAND TRANSMITARRAY UNIT

A. GEOMETRY

The structure of the proposed wideband transmitarray unit is shown in Fig. 1. The proposed TA unit is composed of three layers of metals and three layers of substrates that are Rogers RO4003C ($\varepsilon_r = 3.55$, $\tan\delta = 0.0027$). The period length of the square wideband TA unit is $P = 7$mm $(0.35\lambda_0)$, the thickness of the substrate is $H = 0.5$mm, $(0.025\lambda_0)$, and there is an air layer with height of $H1$=0.9mm $(0.045\lambda_0)$ between each substrate. The first layer and the third layer have the same patch, and the length of the patch is L. The middle layer of the unit is a Jerusalem slot in the ground. The length of Jerusalem slot is $S = 1.2 * L$ mm, the width of slot is w =0.18mm, the length of branch of Jerusalem slot is $L1 = L$-1mm, and the width of branch slot is $w = 0.18$mm. The introduction of the branch is to increase the phase change of unit.

B. FREQUENCY RESPONSE

The transmitarray is composed of periodically arranged transmitarray units, so periodic boundary conditions are used in

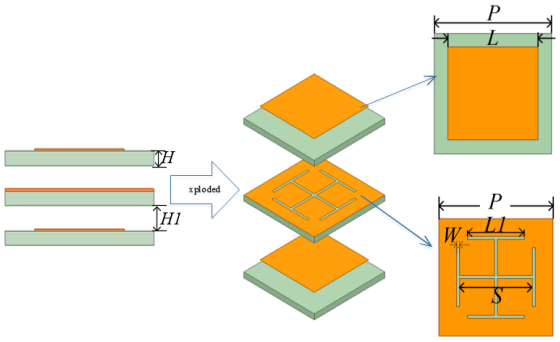

FIGURE 1. 3-D exploded view and parameter definition of the wideband unit.

the full wave simulation software (HFSS) to consider the mutual coupling between units. TM(TE)mode is set on the port to simulate the performance of the unit under x(y) polarization. Fig.2 shows the transmission coefficients and reflection coefficients of the wideband TA unit at x and y polarization, and the S parameters of the wideband TA unit are relatively consistent under the two linear polarization. In the Ku-band (12GHz-18GHz), the insertion loss of the TA unit is less than 0.5dB, and the reflection magnitude is below −10dB. The wideband transmitarray unit has a completely symmetrical structure, and it can be seen from Fig.2 that the wideband unit has the same performance under x and y polarization. In addition, the circularly polarized wave can be decomposed into a combination of linearly polarized waves. Therefore, in the following, only the performance of the transmitarray unit at y polarization is given.

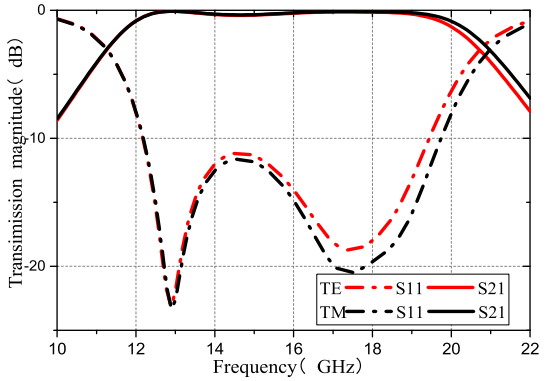

FIGURE 2. Transmission and reflection magnitude of the unit at x and y polarization.

Fig.3 shows the transmission magnitude and phase of the wideband TA unit with different L sizes. As shown in the figure, when L changes from 2.8 mm to 4.6 mm, the unit can obtain 360° phase shift, and the phase curve changes gently. Fig.4 shows the transmission magnitude and phase of the wideband TA unit at different frequencies when varying the length L. The phase curves are parallel in the band from 14GHz to 18GHz, so the designed transmitarray has a wideband response. In general, the transmitarray needs to work at

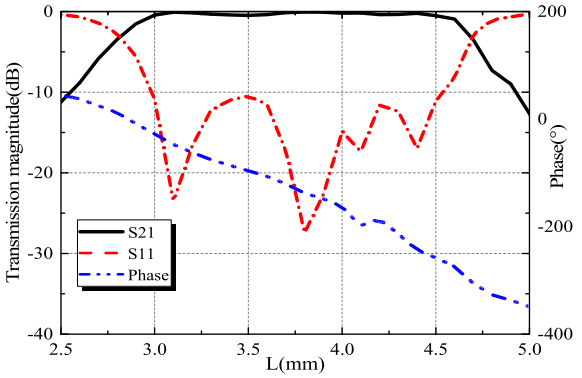

FIGURE 3. Phase and transmission coefficient of the unit at 15GHz.

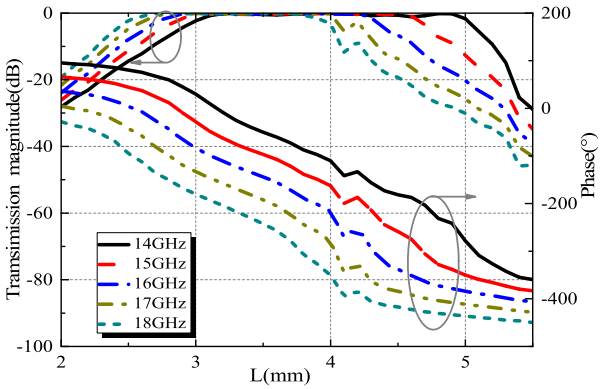

FIGURE 4. Simulated transmission magnitude and phase of the unit at different frequencies.

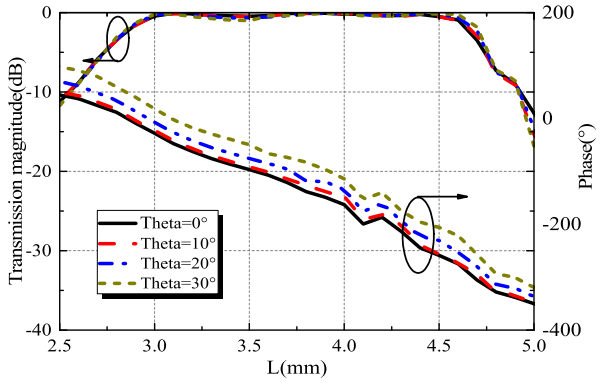

FIGURE 5. Simulated transmission magnitude and phase of the unit with different incident angles at 15GHz.

different incident angles, so it's very important to analyze the characteristics of the TA unit at different incident angles. The transmission magnitude and phase of the wideband TA unit at different incident angles are depicted in Fig.5. The insertion loss is 0.9dB at 30° incident angle. The phase curves of the TA unit when varying the length L are parallel at different incident angles.

Compared with the $0.25\lambda_0$ air layer of TA unit in the previous design, the proposed wideband transmitarray unit introduces an ultra-thin air layer ($0.045\lambda_0$), which is to achieve impedance matching between each layer of the unit. Therefore, the bandwidth of TA unit is expanded and the reflection

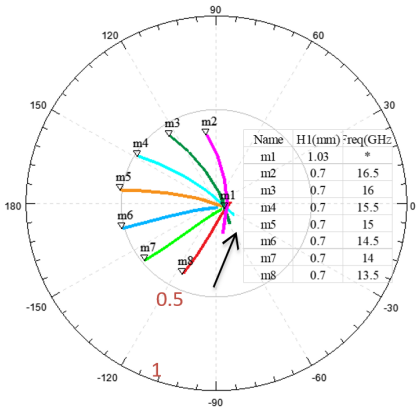

FIGURE 6. Smith chart of the unit with different air layer heights at different frequencies.

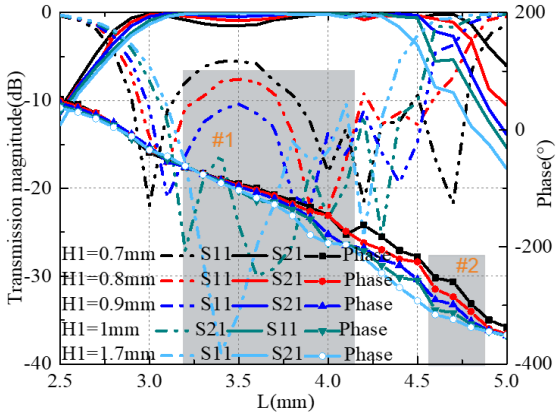

FIGURE 7. Simulated transmission magnitude and phase of the unit with different H1 at 15GHz.

is reduced. The smith chart of transmitarray unit with different air layer heights at different frequencies is depicted in Fig.6. At the same frequency, the higher the air layer is, the closer S11 is to the dot. Therefore, the transmitarray has better transmission characteristics at high heights. The height of the air layer at the convergence point of the curve in the figure is 1.03mm.

Fig.7 shows the transmission magnitude and phase with different heights of the air layer. From the simulation results, the thinner the air layer, the larger the phase compensation range of the TA unit. The phase shift range of $H1$=0.7mm is 33° larger than that of $H1$=1.1mm (#2). However, in the area where L changes from 3mm to 4mm (#1), the thinner the air layer, the higher the reflection magnitude of the TA unit, which will cause serious backward radiation of the transmitarray and reduce the gain of the transmitarray. Therefore, considering the phase shift and transmission amplitude of the unit, the air layer thickness is finally selected as $H1$=0.9mm.

III. DESIGN AND MEASUREMENT OF THE WIDEBAND TRANSMITARRAY

A. DESIGN

Due to the wave path difference between the feed and each unit of the TA array, there is a spatial phase difference

between the unit of the transmitarray. Therefore, in order to obtain a high-gain beam, the spherical wave of the feed needs to be adjusted to a uniform plane wave through the transmitarray. The phase required for each unit of the TA $\bar{r}_0$ array are as follows:

$$\varphi_{ij} = k\left(R_{ij} - \vec{\boldsymbol{r}}_{\boldsymbol{ij}} \cdot \hat{\boldsymbol{r}}_{\mathbf{0}}\right) + \varphi_0 \tag{1}$$

where φ_{ij} is the required transmission phase for the ijth unit, k is the propagation constant, R_{ij} is the distance from the ijth unit to the feed, $\vec{\boldsymbol{r}}_{\boldsymbol{ij}}$ is the position vector of the ijth unit, $\hat{\boldsymbol{r}}_{\mathbf{0}}$ is the main beam unit vector, and φ_0 is a phase constant, as shown in Fig.8. In order to reduce the influence of low transmission magnitude unit at transmitarray, the units in the central region is generally selected with good transmission performance. Such a transmitarray has better working characteristics, such as high transmission ability, broadband, etc.

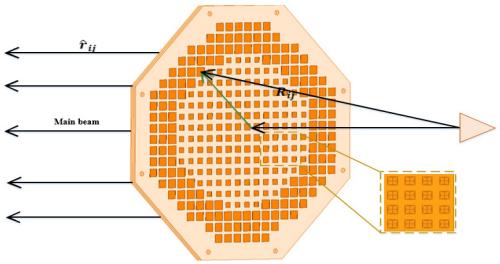

FIGURE 8. Schematic view of the wideband transmitarray.

Aperture efficiency is an important performance index of transmitarray antenna. In order to improve the aperture efficiency of the transmitarray antenna and reduce the spillover loss, the appropriate focal diameter ratio (the ratio of the distance from the feed to the transmitarray and the diameter of the transmitarray) should be selected in the design process. The phase of each unit is compensated accurately to make the phase distribution of array aperture consistent so as to achieve maximum gain.

B. SIMULATION AND MEASUREMENT

The overall schematic diagram of the proposed wideband transmitarray is shown in Fig.8. The array is composed of multilayer structure, which is a two-dimensional periodic arrangement of subwavelength structural units. The shape of the transmitarray is an equivalent circle, which is consists of 351 units, and the radius of the transmitarray is 70mm. The overall thickness is $0.165\lambda_0$. The distance from the feed horn to the center of the array is 105mm, and the focal diameter ratio of the transmitarray is 0.75. The selection principle of focal diameter ratio is that the electric field level at the edge of the array is 10 dB lower than that at the center of the transmitarray. The gain of the feed horn is 15.6dBi at 15GHz.

Fig.9 shows the fabricated of the proposed wideband transmitarray. The full wave simulation results are obtained using HFSS, and the measurement results in microwave anechoic chamber are also provided, which are shown in Fig.10, 11 and 12. These figures confirm the agreement between the

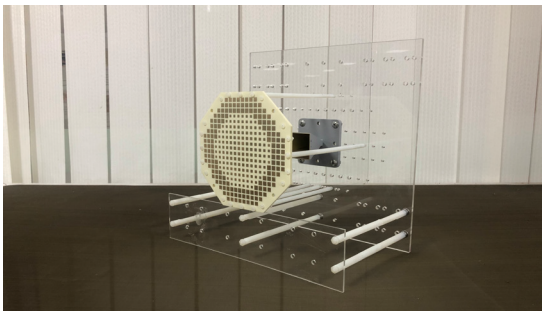

FIGURE 9. Fabricated prototype of the wideband transmitarray.

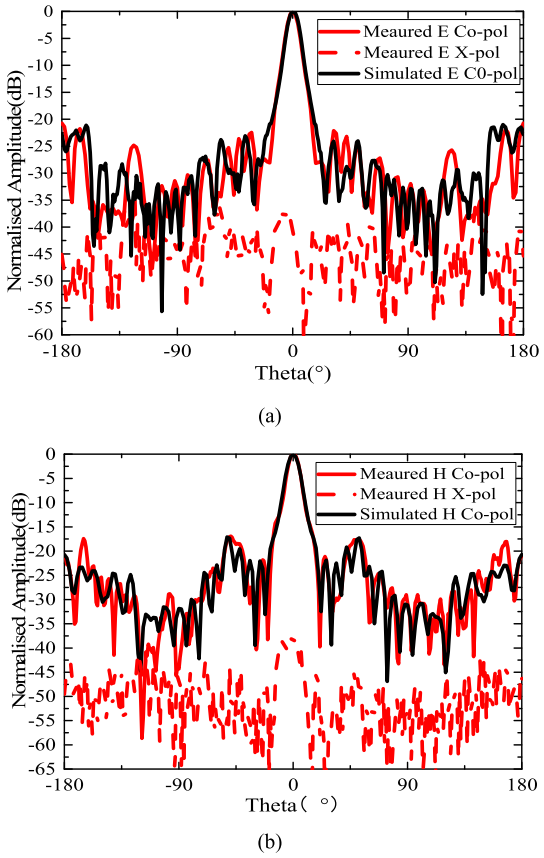

FIGURE 10. Simulated and measured normalized radiation patterns at 15 GHz (a) E-plane and (b) H-plane.

simulation results and the measurement results. Fig.10 provides the radiation patterns of transmitarray antenna in E-plane and H-plane at 15GHz, and the SLL is lower than 16dB. The sidelobe of the measured radiation pattern is higher than that of simulation, which is caused by machining error and human error during assembly. The measured cross-polarization level of the wideband transmitarray is higher than 35dB. Since the ideal feed horn is used in the simulation, the cross-polarization level of the simulation will be more than 50dB. Therefore, the cross-polarization level of the simulation is not given in Fig.10. The simulated and measured gain variation of the transmitarray within its operating frequency band are depicted in Fig.11. The measurement results show that the 1-dB gain bandwidth of the array is 37.3%

TABLE 1. Comparison of the Proposed Transmitarray With Referenced Transmitarray.

Ref.	Frequency	Thickness (λ_0)	Array Size (λ_0^2)	Polarization	Gain(dB)	Aperture Efficiency (%)	1-dB Gain BW (%)
[8]	13.5 GHz	0.360	4×4	Dual LP & Dual CP	22.0	60	16
[11]	11.0 GHz	0.222	10×10	Single LP	27.2	55.71	24.1
[21]	12.0 GHz	0.127	5.6×5.6	Single LP	21.9	40	21.5
[24]	21.0 GHz	0.140	14×14	Dual LP	20.0	40	9.6
[25]	11.0 GHz	0.220	8.8×8.8	Single LP	24.7	40.7	56
This work	15.0 GHz	0.165	$\pi * (3.5)^2$	Dual LP & Dual CP	23.06	42.3	37.3

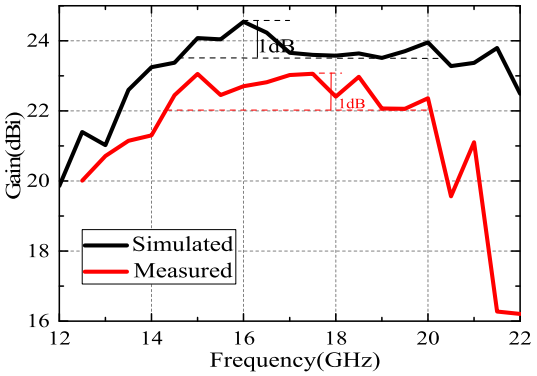

FIGURE 11. Measured and simulated gains versus frequency.

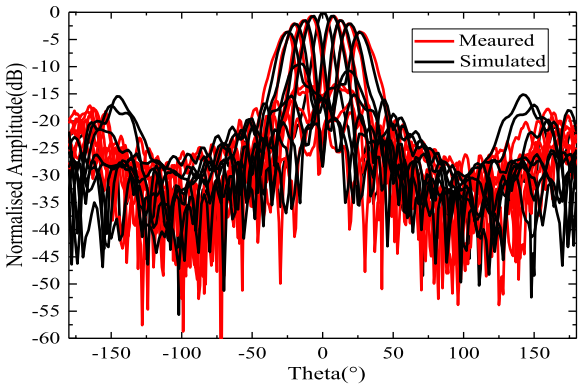

FIGURE 12. Simulated and measured normalized scanning radiation pattern.

(14.4GHz-20GHz), and the maximum measurement gain is 23.06dBi. The gain of transmitarray is increased by 7.46dBi relative to the gain of the feed horn at 15GHz. Since the feed of simulation is an ideal horn and processing error, the difference between the simulated and measured gain is 1.8dB. The simulated and measured normalized scanning patterns are shown in Fig.12. When TA array is scanned to $\pm$ 30°, the gain of transmitarray decreases by 3.6dB. Table 1 presents the characteristics of the transmitarray proposed in this article and compares it with the recently published articles on wideband transmitarrays. It can be seen from Table 1 that although the profile of the transmitarray in [21] and [24] is lower than that in this article, the transmitarray in [21] can only work at single linear polarization, and the 1dB gain bandwidth of [24] is only 9.6%. In addition, the 1.5 dB gain bandwidth of the transmitarray in [25] is wider than that in this article, but the transmitarray in [25] can also only work in the single linear polarization. To sum up, the proposed transmitarray has a lower profile and a wider frequency band, and can work in dual linear or dual circular polarization.

IV. CONCLUSION

A low profile wideband transmitarray is proposed, which is composed of periodically arranged transmitarray unit. The wideband transmitarray unit has a symmetrical structure, so the transmitarray antenna can work in dual linear polarization or dual circular polarization. The transmitarray unit can achieve a phase shift of 360° with 3-dB magnitude loss. The overall thickness of the fabricated transmitarray prototype is $0.165\lambda_0$. The measured gain is 23.06 dBi at 15GHz with 42.3% the aperture efficiency. The measured results show that the 1-dB gain bandwidth of the proposed wideband transmitarray is 37.3% (14.4GHz-20GHz).

REFERENCES

[1] L. Dussopt, "Transmitarray antennas," in *Aperture Antennas for Millimeter and Sub-Millimeter Wave Applications*, 1st ed. Cham, Switzerland: Springer, 2018.

[2] Y.-M. Cai, W. Li, K. Li, S. Gao, and Y. Yin, "A novel ultrawideband transmitarray design using tightly coupled dipole elements," *IEEE Trans. Antennas Propag.*, vol. 67, no. 1, pp. 242–250, Jan. 2019.

[3] W. A. Imbriale, S. S. Gao, and L. Boccia, *Space Antenna Handbook*. Hoboken, NJ, USA: Wiley, 2012.

[4] P. Qin, L. Song, and Y. J. Guo, "Beam steering conformal transmitarray employing ultra-thin triple-layer slot elements," *IEEE Trans. Antennas Propag.*, vol. 67, no. 8, pp. 5390–5398, Aug. 2019, doi: 10.1109/TAP.2019.2918496.

[5] C. Tian, Y.-C. Jiao, G. Zhao, and H. Wang, "A wideband transmitarray using triple-layer elements combined with cross slots and double square rings," *IEEE Antennas Wireless Propag. Lett.*, vol. 16, pp. 1561–1564, 2017, doi: 10.1109/LAWP.2017.2651027.

[6] W. An, S. Xu, F. Yang, and M. Li, "A double-layer transmitarray antenna using malta crosses with vias," *IEEE Trans. An-tennas Propag.*, vol. 64, no. 3, pp. 1120–1125, Mar. 2016, doi: 10.1109/TAP.2015.2513427.

[7] L. W. Wu, H. F. Ma, Y. Gou, R. Y. Wu, Z. X. Wang, and M. Wang, "High-transmission ultrathin huygens' metasurface with 360° phase control by using double-layer transmitarray elements," *Phys. Rev. Appl.*, vol. 12, Aug. 2019, Art. no. 024012.

[8] Q. Luo, S. Gao, M. Sobhy, and X. Yang "Wideband transmitarray with reduced profile," *IEEE Antennas Wireless Propag. Lett.*, vol. 17, no. 3, pp. 450–453, Mar. 2018, doi: 10.1109/LAW.P.2018.2794605.

[9] S. H. Ramazannia Tuloti, P. Rezaei, and F. Tavakkol Hamedani, "High-efficient wideband transmitarray antenna," *IEEE Antennas Wireless Propag. Lett.*, vol. 17, no. 5, pp. 817–820, May 2018, doi: 10.1109/LAWP.2018.2817363.

[10] K. Pham, N. T. Nguyen, and A. Clemente, "Design of wideband dual linearly polarized transmitarray antennas," *IEEE Trans. Antennas Propag.*, vol. 64, no. 5, pp. 2022–2026, May 2016, doi: 10.1109/TAP.2016.2536160.
[11] K. Mavrakakis, H. Luyen, J. H. Booske, and N. Behdad, "Wideband transmitarrays based on polarization-rotating miniaturized-element frequency selective surfaces," *IEEE Trans. Antennas Propag.*, vol. 68, no. 3, pp. 2128–2137, Mar. 2020, doi: 10.1109/TAP.2019.2949694.
[12] J. P. Doane, K. Sertel and J. L. Volakis, "A wideband, wide scanning tightly coupled dipole array with integrated balun (TCDA-IB)," *IEEE Trans. Antennas Propag.*, vol. 61, no. 9, pp. 4538–4548, Sep. 2013, doi: 10.1109/TAP.2013.2267199.
[13] H. Zhang, S. Yang, S. Xiao, Y. Chen, S. Qu, and J. Hu, "Ultrawideband phased antenna arrays based on tightly coupled open folded dipoles," *IEEE Antennas Wireless Propag. Lett.*, vol. 18, no. 2, pp. 378–382, Feb. 2019, doi: 10.1109/LAWP.2019.2891892.
[14] H. Zhang, S. Yang, Y. Chen, J. Guo, and Z. Nie, "Wideband dual-polarized linear array of tightly coupled elements," *IEEE Trans. Antennas Propag.*, vol. 66, no. 1, pp. 476–480, Jan. 2018, doi: 10.1109/TAP.2017.2776959.
[15] Z.-W. Miao, Z.-C. Hao, G. Q. Luo, L. Gao, J. Wang, X. Wang, and W. Hong, "140 GHz high-gain LTCC-integrated transmit-array antenna using a wideband SIW aperture-coupling phase delay structure," *IEEE Trans. Antennas Propag.*, vol. 66, no. 1, pp. 182–190, Jan. 2018, doi: 10.1109/TAP.2017.2776345.
[16] C. Jouanlanne, T. Le Nadan, M. Huchard, L. Petit, and A. Clemente, "Design of a linearly-polarized 3-bit transmitarray antenna at 60 GHz," in *Proc. IEEE Int. Symp. Antennas Propag. (APSURSI)*, Fajardo, Puerto Rico, Jun./Jul. 2016, pp. 793–794, doi: 10.1109/APS.2016.7696105.
[17] F. Diaby, A. Clemente, and L. Di Palma, "Wideband circularly-polarized 3-bit transmitarray antenna in Ka-band," in *Proc. 11th Eur. Conf. Antennas Propag. (EUCAP)*, Paris, France, Mar. 2017, pp. 2269–2273, doi: 10.23919/EuCAP.2017.7928661.
[18] C. Jouanlanne, A. Clemente, and M. Huchard, "Wideband linearly polarized transmitarray antenna for 60 GHz backhauling," *IEEE Trans. Antennas Propag.*, vol. 65, no. 3, pp. 1440–1445, Mar. 2017, doi: 10.1109/TAP.2017.2655018.
[19] L. Di Palma, A. Clemente, L. Dussopt, R. Sauleau, P. Potier, and P. Pouliguen, "Circularly polarized transmit-array with sequentially rotated elements in Ka band," in *Proc. 8th Eur. Conf. Antennas Propag. (EuCAP)*, The Hague, The Netherlands, Apr. 2014, pp. 1418–1422, doi: 10.1109/EuCAP.2014.6902046.
[20] F. Zhang, G. Yang, and Y. Jin, "Low-profile circularly polarized transmitarray for wide-angle beam control with a third-order meta-FSS," *IEEE Trans. Antennas Propag.*, vol. 68, no. 5, pp. 3586–3597, May 2020, doi: 10.1109/TAP.2020.2964957.
[21] F. Wu, J. Wang, K. Luk, and W. Hong, "A wideband low-profile efficiency-improved transmitarray antenna with over-1-bit phase-shifting elements," *IEEE Access*, vol. 8, pp. 32163–32169, 2020, doi: 10.1109/ACCESS.2020.2971564.
[22] A. H. Abdelrahman, A. Z. Elsherbeni, and F. Yang, "High-gain and broadband transmitarray antenna using triple-layer spiral dipole elements," *IEEE Antennas Wireless Propag. Lett.*, vol. 13, pp. 1288–1291, 2014, doi: 10.1109/LAWP.2014.2334663.
[23] Q. Luo, S. Gao, M. Sobhy, and X. Yang, "A hybrid design method for thin-panel transmitarray antennas," *IEEE Trans. Antennas Propag.*, vol. 67, no. 10, pp. 6473–6483, Oct. 2019, doi: 10.1109/TAP.2019.2923076.
[24] X. Yi, T. Su, X. Li, B. Wu, and L. Yang, "A double-layer wideband transmitarray antenna using two degrees of freedom elements around 20 GHz," *IEEE Trans. Antennas Propag.*, vol. 67, no. 4, pp. 2798–2802, Apr. 2019, doi: 10.1109/TAP.2019.2893265.
[25] P. Feng, S. Qu, and S. Yang, "Octave bandwidth transmitarrays with a flat gain," *IEEE Trans. Antennas Propag.*, vol. 66, no. 10, pp. 5231–5238, Oct. 2018, doi: 10.1109/TAP.2018.2858198.

MEI-YU LI was born in Henan, China, in June 1995. She received the B.S. degree in communication engineering from the North China University of Water Resources and Electric Power, Zhengzhou, China, in 2018. She is currently pursuing the M.S. degree with the University of Electronic Science and Technology of China (UESTC), Chengdu, China. Her current research interests include multibeam antennas, reconfigurable antennas, metasurface antennas, and phased arrays.

YONG-LING BAN (Member, IEEE) was born in Henan, China. He received the B.S. degree in mathematics from Shandong University, in 2000, the M.S. degree in electromagnetics from Peking University, in 2003, and the Ph.D. degree in microwave engineering from the University of Electronic Science and Technology of China (UESTC), in 2006. In July 2006, he joined as a Microwave Engineer of the Xi'an Mechanical and Electric Information Institute. He joined Huawei Technologies Company, Ltd., Shenzhen, China. At Huawei, he designed and implemented various terminal antennas for 15 data card and mobile phone products customized from leading telecommunication industries like Vodafone. From May 2014 to April 2015, he visited the Queen Mary University of London as a Scholar Visitor. From September 2010 to July 2016, he was an Associate Professor with UESTC, where he is currently a Professor. He has authored more than 110 referred journal and conference articles on these topics. He holds 20 granted and pending Chinese and overseas patents. His research interests include wideband small antennas for 4G/5G handset devices, MIMO antenna, and millimeter wave antenna array.

FU-QIANG YAN was born in Jilin, China, in October 1986. He received the B.S. degree in detection guidance and control technology from the Beijing University of Aeronautics and Astronautics, Beijing, China, in 2009. He is currently pursuing the M.S. degree with the University of Electronic Science and Technology of China (UESTC), Chengdu, China. He also works at the Army Armoured Corps College Non-commissioned Officer School. His current research interest includes MIMO antenna.